J Mater Sci (2014) 49:7099–7104
DOI 10.1007/s10853-014-8416-8

Structural and magnetic properties of $(Cr_{1-x}Mn_x)_5Al_8$ solid solution and structural relation to hexagonal nanolaminates

A. Mockute · P. O. Å. Persson · J. Lu · A. S. Ingason · F. Magnus · S. Olafsson · L. Hultman · J. Rosen

Received: 31 March 2014 / Accepted: 21 June 2014 / Published online: 15 July 2014

Abstract Electron microscopy is used to reveal the competitive epitaxial growth of bcc structure $(Cr_{1-x}Mn_x)_5Al_8$ and $(Cr_{1-y}Mn_y)_2AlC$ [$M_{n+1}AX_n$ (MAX)] phase during both magnetron sputtering and arc deposition. X-ray diffraction θ–2θ measurements display identical peak positions of (000n)-oriented MAX phase and $(Cr_{1-x}Mn_x)_5Al_8$, due to the interplanar spacing of $(Cr_{1-x}Mn_x)_5Al_8$ that matches exactly half a unit cell of $(Cr_{1-y}Mn_y)_2AlC$. Vibrating sample magnetometry shows that a thin film exclusively consisting of $(Cr_{1-x}Mn_x)_5Al_8$ exhibits a magnetic response, implying that the potential presence of this phase needs to be taken into consideration when evaluating the magnetic properties of $(Cr, Mn)_2AlC$.

Introduction

The $M_{n+1}AX_n$ (MAX) phases constitute a class of layered solids, where M denotes an early transition metal, A denotes an A-group element, X denotes C or N, and n = 1-3 [1]. These inherent atomic laminates have a hexagonal structure, belonging to the $P6_3/mmc$ space group, which for $n = 1$ corresponds to a M–X–M–A–M–X–M–A atomic layer stacking in the c-direction. More than 60 MAX phases have been synthesized to date, and the materials have attracted attention primarily due to the unique combination of metallic (good electrical and thermal conductors) and ceramic (hard, oxidation, and wear resistant) characteristics, as well as extreme damage tolerance [2].

Research on MAX phase thin films has mostly been concentrated on epitaxial growth with the c-axis perpendicular to the substrate surface and subsequent materials characterization. Phase identification and evaluation of the film quality often relies on fast, simple, and nondestructive X-ray diffraction (XRD) measurements, and in particularly symmetric θ–2θ scans.

In a symmetric θ–2θ configuration, atomic planes perpendicular to the diffraction vector q are probed. For polycrystalline samples, where grains are randomly oriented, peaks from all crystallographic planes are observed and form a unique XRD θ–2θ pattern, leading to straightforward phase identification. However, thin films are often highly textured, such that a θ–2θ scan returns a limited set of crystallographic planes. For the case of a sample containing two epitaxial phases with identical out-of-plane spacings, the XRD θ–2θ scan exhibits overlapping peaks at exactly the same positions. Consequently, correct phase identification is challenging. Hence, undiscovered competing phases attained within the M–A–X elemental system could have drastic consequences on stated sample phase purity, interpretation of experimental data, and result in divergence in reported results.

We present experimental evidence of the formation of bcc $(Cr_{1-x}Mn_x)_5Al_8$ ($x = 0.72$) as a competing phase during the synthesis of the $(Cr, Mn)_2AlC$ MAX phase. Furthermore, it is shown that epitaxial films of $(Cr, Mn)_2AlC$, Cr_5Al_8 and Mn_5Al_8 as well as $(Cr, Mn)_5Al_8$ provide

A. Mockute (✉) · P. O. Å. Persson · J. Lu · A. S. Ingason · L. Hultman · J. Rosen
Thin Film Physics Division, Department of Physics, Chemistry, and Biology (IFM), Linköping University, 581 83 Linköping, Sweden
e-mail: aurmo@ifm.liu.se

F. Magnus
Department of Physics and Astronomy, Uppsala University, Box 530, 751 21 Uppsala, Sweden

S. Olafsson
Science Institute, University of Iceland, Dunhaga 3, 107 Reykjavík, Iceland

identical XRD θ–2θ scans with respect to peak positions. Magnetic properties have previously been theoretically predicted for the (Cr, Mn)$_2$AlC MAX phase [3]. In order to investigate the possible influence of a (Cr, Mn)$_5$Al$_8$ phase on the magnetic response, (Cr, Mn)$_5$Al$_8$ as well as Mn$_5$Al$_8$ has also been characterized with respect to magnetic properties. Moreover, we emphasize XRD pole measurements as the correct approach to enable the detection of competing phases.

Experimental details

Thin film synthesis of (Cr, Mn)$_2$AlC MAX phase was attempted using high current pulsed cathodic arc and DC magnetron sputtering. For arc depositions, compound Cr/Mn (50/50 at.%) as well as elemental Al and C cathodes was used in alternating mode at a rate of 10 Hz. Pulse lengths were set to 450, 250, and 1000 μs for Cr/Mn, Al, and C cathodes, respectively. The films were deposited on Al$_2$O$_3$(0001) substrates at a base pressure of 5×10^{-7} Torr and at a growth temperature of 625 °C. Magnetron sputtering was performed from Cr/Mn (50/50 at.%), Al, and C targets at a base pressure of 3×10^{-7} Torr at 600 °C on Al$_2$O$_3$(0001) and MgO(111) substrates.

Cr$_2$AlC, Cr$_5$Al$_8$, Mn$_5$Al$_8$, and (Cr$_{0.28}$Mn$_{0.72}$)$_5$Al$_8$ films were deposited on Al$_2$O$_3$(0001) substrates by DC magnetron sputtering from elemental targets at a base pressure of 9×10^{-8} Torr at the growth temperature of 600 °C. All substrates were cleaned in acetone, methanol, and isopropanol ultrasonic baths for 10 min each and degassed for 10 min at the growth temperature prior to deposition.

X-ray diffraction characterization was performed using a Panalytical Empyrian MRD equipped with a line focus Cu Kα source ($\lambda = 1.54$ Å) and a hybrid mirror optics on the incident beam side for θ–2θ measurements. Pole scans were acquired with point focus and X-ray lens optics. Scanning electron microscopy (SEM) analysis was conducted using a LEO 1550 SEM. Cross-sectional and plan-view samples for transmission electron microscopy (TEM) analysis were prepared by conventional mechanical methods followed by low-angle ion milling with a final fine-polishing step at low acceleration voltage. TEM imaging, electron diffraction (ED), and energy-dispersive X-ray spectroscopy (EDX) for elemental analysis were performed in a Tecnai G2 TF20 UT FEG instrument operated at 200 kV, equipped with an EDX detector, while scanning (S)TEM imaging and EDX mapping were performed in the doubly corrected Linköping Titan^3 60–300 equipped with a Super-X EDX detector. Magnetic characterization was carried out in a Cryogenic Ltd. vibrating sample magnetometer (VSM).

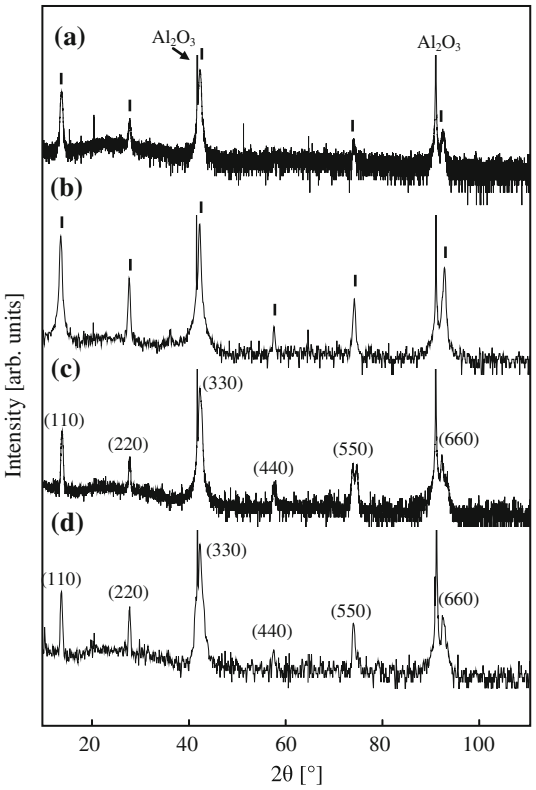

Fig. 1 XRD θ–2θ scans of thin films resulting from attempted (Cr, Mn)$_2$AlC MAX phase synthesis by **a** cathodic arc and **b** magnetron sputtering. Indicated peak positions correspond to the (000n) MAX phase. **c** Cr$_5$Al$_8$ and **d** Mn$_5$Al$_8$ θ–2θ scans from magnetron sputtered films

Results and discussion

Structural and compositional analysis

Figure 1a, b presents XRD θ–2θ scans of thin films aimed for (Cr, Mn)$_2$AlC MAX phase by cathodic arc and magnetron sputtering, respectively, on Al$_2$O$_3$(0001) substrates. Only peaks corresponding to (000n) Cr$_2$AlC positions are observed, suggesting films consisting of phase pure epitaxial MAX phase. It was previously reported that the c-lattice constant remains unaffected upon Mn incorporation, and thus, shifts in peak positions are not expected [4].

The cathodic arc-deposited sample was subjected to high-resolution (HR) STEM imaging. Apart from a significant component of (Cr, Mn)$_2$AlC, the sample also exhibits an unknown structure, which is shown in Fig. 2. While the discrete atomic organization of the structure, as shown in Fig. 2a, does not resemble a MAX phase, the laminated appearance is identical to a MAX phase structure. The insets in both (a) and (b) show the intensity line profile of the structure along the growth direction. As for a MAX phase, the structure exhibits two bright layers of heavier elements (compared with the M$_2$X layers in a MAX phase), which are interleaved by a lighter element

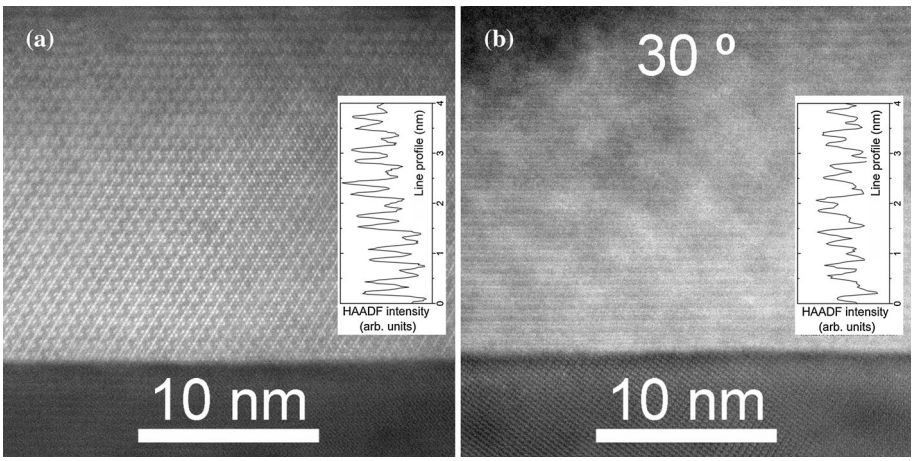

Fig. 2 **a** High-resolution cross-sectional STEM imaging along the [1$\bar{1}$00] MAX phase zone axis, including intensity line profile, showing a laminated appearance identical to a MAX phase structure. **b** In-plane rotated sample (30°) to the [2$\bar{1}\bar{1}$0] zone axis of the MAX phase structure

layer (compared with the MAX phase *A* layer). The in-plane rotated sample, see Fig. 2b, also exhibits the same layered structure.

The layered structure shown in Fig. 2 is further investigated in Fig. 3. A low-magnification STEM image of a deposited film particle is shown in Fig. 3a. Elemental mapping of the particle reveals two domains of different composition, where the composition of the left domain is Cr/Mn/Al with approximate ratio of 9:22:69. The structure of the left part of the particle corresponds to that shown in Fig. 2, while the right domain corresponds to the (Cr, Mn)$_2$AlC MAX phase structure shown in Fig. 3b by HRSTEM. The interface between the two domains is further shown in (c). Note the transition where the atomic layers bridge seamlessly between the domains, as indicated by the arrows in Fig. 3c. Even the contrasts of the layers are perfectly matched (bright–bright and dark–dark). The only distinction between the domains can be made from the discrete hexagonal (zigzag) atomic pattern of the MAX phase (right) to the continuous lines of the competing phase (left). The perfect transition between the domains, shown at high magnification in Fig. 3c, is remarkable. Notably, the atomic layers continue from one domain to the other despite the significant change in composition. This HRSTEM image provides a visual explanation why the presence of this second commensurate phase may be overlooked in the XRD measurements shown in Fig. 1a, b. As distances along the diffraction vector q are probed in θ–2θ configuration, equal distances give rise to peaks at the same 2θ angles and hence, peak overlap.

The domains in this sample proved too small to enable ED exclusively on the unknown phase. Therefore, a thin film aiming for the measured composition was synthesized. TEM–EDX analysis of the resulting film proved the attained composition of Cr/Mn/Al equal to 9:22:69. HRTEM and ED were subsequently performed on the film to obtain structural information and crystallographic

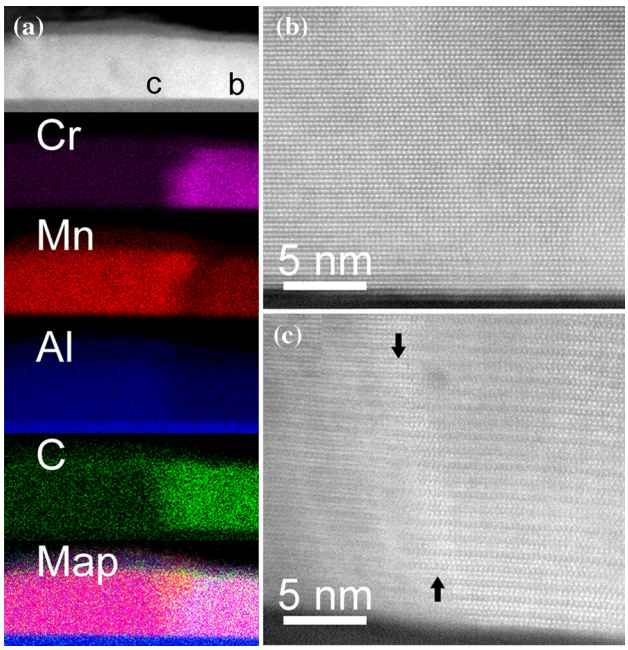

Fig. 3 **a** STEM cross-sectional image from the cathodic arc-deposited film with corresponding EDX elemental maps of Cr, Mn, Al, and C, **b** HRSTEM image of the (Cr, Mn)$_2$AlC MAX phase structure, and **c** HRSTEM image of the interface between the domains

relation with the substrate. Figure 4a–f presents ED and corresponding filtered HRTEM images along [001], [111], and [113] zone axes. The structure could be identified as a bcc crystal structure with lattice constant of 9.05 Å, with an out-of-plane relation to the substrate as bcc(110)// Al_2O_3(0001).

Plan-view TEM and ED analyses of the [(Cr, Mn)$_2$ AlC + bcc structure] film grown on MgO(111), shown in Fig. 5, reveal that the grains of the unknown phase acquire three different in-plane orientations, with ~120° in between.

According to the literature, Cr_5Al_8 and Mn_5Al_8 are phases exhibiting a bcc structure with a lattice constant

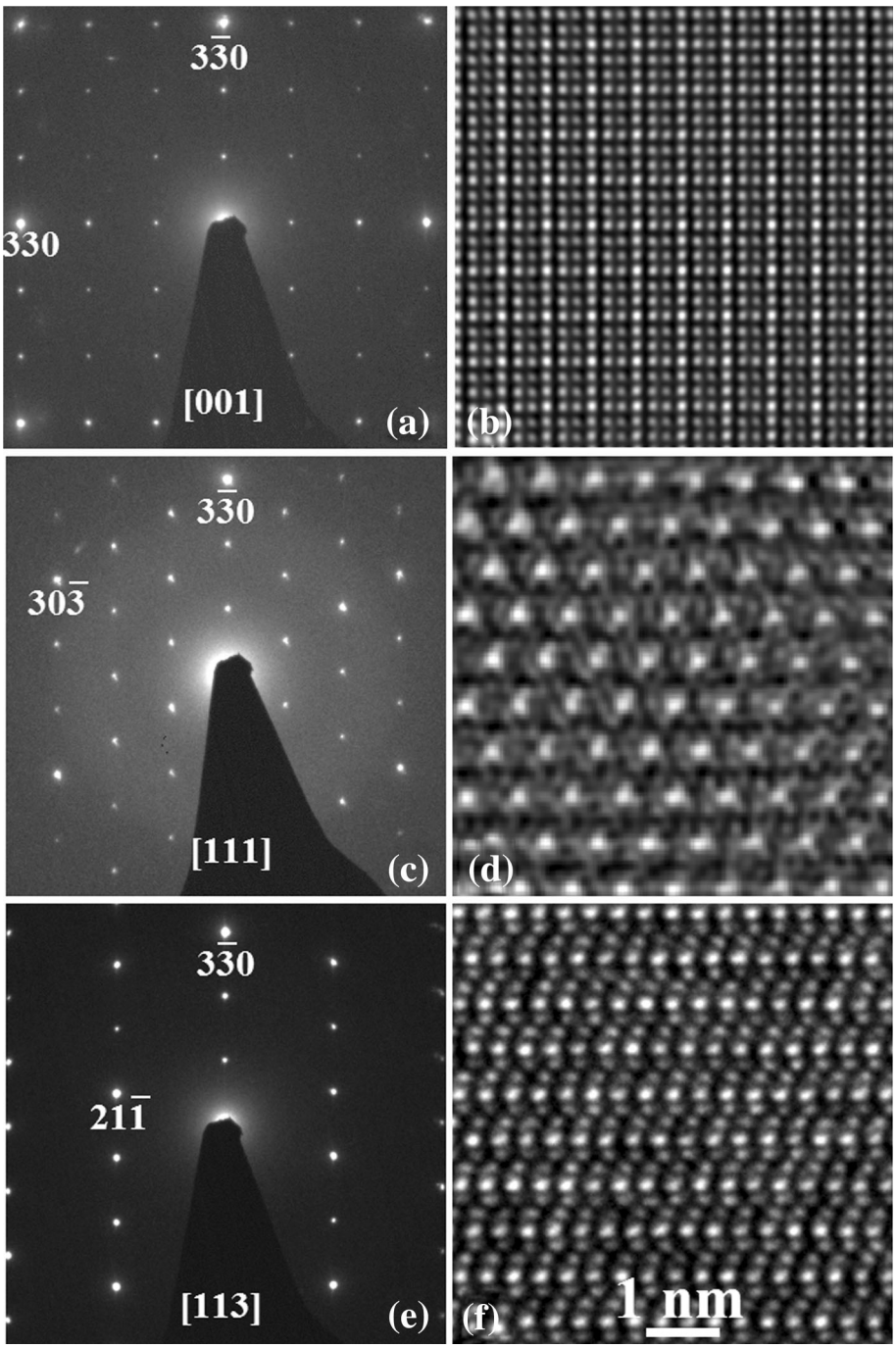

Fig. 4 ED and corresponding filtered HRTEM of the unknown phase along **a**, **b** [001], **c**, **d** [111], and **e**, **f** [113] zone axes

of approximately 9 Å. Both have been experimentally realized [5, 6], and according to the phase diagram, they can form a solid solution $(Cr_{1-x}Mn_x)_5Al_8$. Considering the here-attained composition of the unknown bcc structure, it would correspond to $(Cr_{0.28}Mn_{0.72})_5Al_8$. Both Cr_5Al_8 and Mn_5Al_8 were synthesized for further XRD analysis, and in Fig. 1c, d, θ–2θ measurements of Cr_5Al_8 and Mn_5Al_8, respectively, are presented. The resulting XRD scans are strikingly similar to the (Cr, Mn)$_2$AlC. In fact, the peaks appear at exactly the same positions (13.8°, 27.7°, 42.2°, 57.2°, 73.7°, and 92.1°) for all three phases. It is obvious that by means of XRD θ–2θ measurement, (Cr, Mn)$_2$AlC and $(Cr_{1-x}Mn_x)_5Al_8$ cannot be distinguished, which implies that previous studies may contain undiscovered competing phases coexisting with the MAX phase, or, in the extreme case, a sample with no actual MAX phase can be misinterpreted as phase pure MAX.

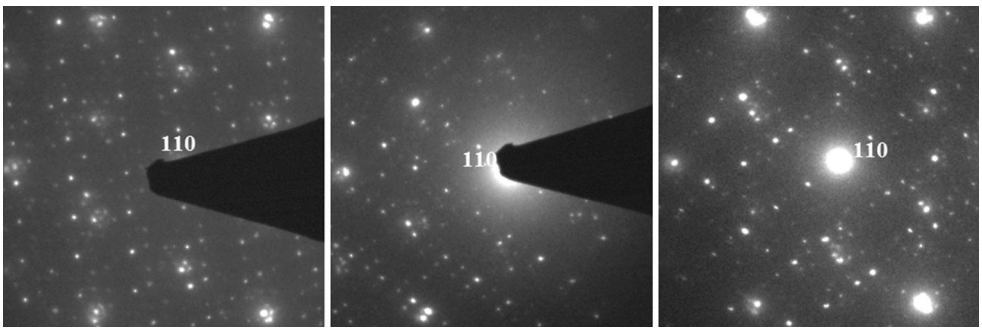

Fig. 5 ED of a plan-view [$(Cr, Mn)_2AlC$ + bcc structure] sample on MgO(111). Diffraction pattern is recorded along [110] zone axis of the unknown phase. Three different in-plane orientations of the bcc structure can be identified

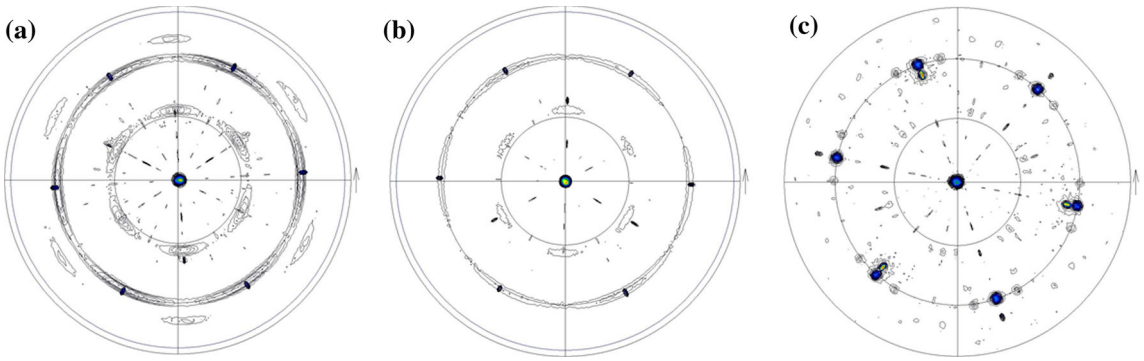

Fig. 6 Pole figures of **a** $Cr_5Al_8(110)//Al_2O_3(0001)$, **b** $Mn_5Al_8(110)//Al_2O_3(0001)$, and **c** [$(Cr, Mn)_2AlC(0001)$ + $(Cr, Mn)_5Al_8(110)$]// MgO(111) at $2\theta = 42.3°$ corresponding to (411) planes for tilt angle $\psi = [0–88]°$. Sixfold symmetry at 33.5°, 60°, and 70.3° confirms the bcc crystal structure of $(Cr, Mn)_5Al_8$

Pole measurements were taken to find an alternative approach to distinguish between the MAX phase and $(Cr, Mn)_5Al_8$. In Cr_5Al_8 and Mn_5Al_8 as well as [$(Cr, Mn)_2AlC$ + $(Cr, Mn)_5Al_8$]//MgO, the bcc (411) planes at $2\theta = 42.3°$ were mapped for tilt angle $\psi = [0–88]°$. In Fig. 6a–c, sixfold symmetry at 33.5°, 60°, and 70.3° is observed, corresponding to angles between (110) and (411) planes in bcc crystal structure. However, the relatively weak peaks at 70.3° are not visible in the Mn_5Al_8 scan, which displays overall lower intensities. Corresponding measurements of an epitaxial phase pure $(Cr, Mn)_2AlC$ film would only provide a sixfold symmetric $(10\bar{1}3)$ peak at $\psi \approx 60°$. Consequently, the middle peak at $\psi = 60°$ in Fig. 6c is an overlap of $(Cr, Mn)_2AlC$ and $(Cr, Mn)_5Al_8$. The high-intensity peaks at $\psi = 37.8°$ and 61° in Fig. 6a, b originate from Al_2O_3 substrate, while in Fig. 6c MgO substrate is visible as threefold symmetric peak at $\psi = 54.4°$. It is interesting to note that the peaks are broadened when Al_2O_3 is used as substrate, while for MgO they are grouped in three, indicating better epitaxial match on MgO than on Al_2O_3 and three in-plane orientations, in agreement with observations in TEM.

Other MAX phase systems can also contain competing phases involving *M* and *A* elements that crystallize in the here-reported bcc structure. One such example is V_5Al_8. Hence, it is recommended to interpret XRD θ–2θ measurements of V_2AlC with great care.

Magnetic properties

Recently, $(Cr,Mn)_2GeC$ [7, 8], $(Cr,Mn)_2AlC$ [9], and Mn_2GaC [10] have been reported as the first magnetic MAX phases. $(Cr,Mn)_2AlC$ has now been characterized. Phase purity is extremely important for correct analysis of magnetic characterization data, and the presence of undiscovered magnetic impurity phases may lead to false conclusions. Therefore, we took VSM measurements on the $(Cr, Mn)_5Al_8$ and Mn_5Al_8 samples.

Figure 7 shows the in-plane magnetization of the $(Cr_{0.28}Mn_{0.72})_5Al_8$ and Mn_5Al_8 thin films as a function of magnetic field at 10 K. The magnetic signal from Mn_5Al_8 is weak, with the saturation magnetization one-eighth that of $(Cr, Mn)_5Al_8$. The more pronounced magnetic response observed in $(Cr, Mn)_5Al_8$ may be explained by the Cr–Mn exchange interaction. The saturation magnetic moment per *M*-atom at 10 K is 0.16 and 0.03 μ_B for $(Cr, Mn)_5Al_8$ and Mn_5Al_8, respectively, and did not change significantly in the investigated temperature range of 10–300 K. As a

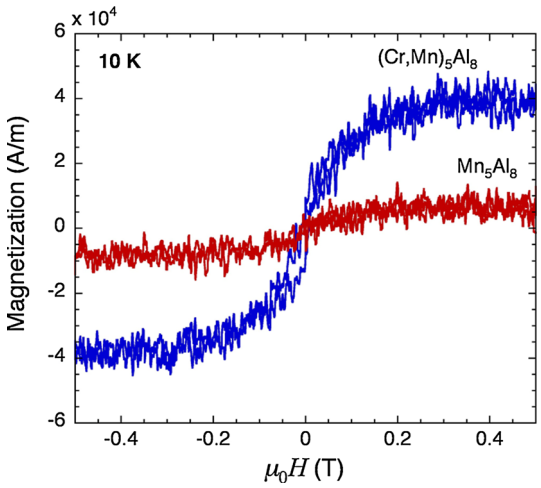

Fig. 7 Magnetic response of the $(Cr_{0.28}Mn_{0.72})_5Al_8$ and Mn_5Al_8 thin films measured by VSM at 10 K with the magnetic field applied parallel to the film plane. The diamagnetic contribution from the Al_2O_3 substrates has been subtracted. The saturation magnetic moment per *M*-atom in $(Cr_{0.28}Mn_{0.72})_5Al_8$ has been determined to 0.16 μ_B. The magnetic signal of Mn_5Al_8 is considerably weaker

magnetic response is observed for (Cr, Mn)$_5$Al$_8$ as well as Mn_5Al_8, it is highly recommended to use complementary analysis techniques for detailed evaluation of phases present and nonlocal composition of the material, prior to characterization of magnetism in (Cr, Mn)$_2$AlC MAX phases. It should be stressed that for the other reported Mn-containing MAX phases (Cr, Mn)$_2$GeC [7, 8] and Mn_2GaC [10], corresponding bcc structures with a $\approx$9 Å do not exist. Furthermore, the formation of these MAX phases has been confirmed by HRSTEM in combination with local composition analysis by EDX. Consequently, the magnetic response stated in these previous reports can be safely ascribed to originate from the MAX phases.

Conclusions

We have presented evidence for a $(Cr_{1-x}Mn_x)_5Al_8$ intermetallic phase of bcc structure and with an interplanar spacing matching exactly half a unit cell of the $(Cr_{1-y}Mn_y)_2AlC$ MAX phase. Hence, routinely performed XRD θ–2θ measurements display peak positions of (000*n*)-oriented MAX phase and $(Cr_{1-x}Mn_x)_5Al_8$, which are identical. Complementary analysis techniques resolving both structure and composition must therefore be used for unambiguous phase identification, as proven here with electron microscopy and diffraction, as well as X-ray pole figure measurements. Furthermore, analysis of magnetic properties of $(Cr_{0.28}Mn_{0.72})_5Al_8$ and Mn_5Al_8 reveals that they are both magnetic, and with a magnetic moment of 0.16 μ_B per *M*-atom at 10 K in $(Cr_{0.28}Mn_{0.72})_5Al_8$. Consequently, possible presence of these phases needs to be taken into consideration when evaluating magnetic properties in both (Cr, Mn)$_2$AlC and related MAX phases.

Acknowledgements The research leading to these results has received funding from the European Research Council under the European Communities Seventh Framework Programme (FP7/2007-2013)/ERC Grant Agreement No. [258509]. J. R. acknowledges funding from the Swedish Research Council (VR) Grant No. 642-2013-8020 and the KAW Fellowship program. P. O. Å. P. and L. H. acknowledge the Swedish Research Council (VR) and Knut and Alice Wallenberg Foundation for providing funding for the Linköping double-corrected Titan^3 60–300 kV electron microscope. J. R. and P. O. Å. P acknowledge support from the SSF Synergy Grant FUNCASE Functional Carbides and Advanced Surface Engineering. F. M. acknowledges financial support from the Carl Trygger Foundation.

References

1. Nowotny H (1970) Struktuchemie einiger Verbindungen der U-bergangsmetalle mit den Elementen C, Si, Ge, Sn. Prog Solid State Chem 2:27–62
2. Barsoum MW (2000) The $M_{(N+1)}AX_{(N)}$ phases: a new class of solids. Prog Solid State Chem 28:201–281
3. Dahlqvist M, Alling B, Abrikosov IA, Rosen J (2011) Magnetic nanoscale laminates with tunable exchange coupling from first principles. Phys Rev B 84(22):220403
4. Mockute A, Dahlqvist M, Emmerlich J, Hultman L, Schneider JM, Persson POÅ, Rosen J (2013) Synthesis and ab initio calculations of nanolaminated (Cr, Mn)$_2$AlC compounds. Phys Rev B 87:094113
5. Braun J, Ellner M, Predel B (1992) Zur Struktur der Hochtemperaturphase Cr_5Al_8(h). J Alloy Compd 183:444–448
6. Grushko B, Stafford GR (1989) A structural study of a metastable bcc phase in Al–Mn alloys electrodeposited from molten salts. Scr Metall 23:557–562
7. Ingason AS, Mockute A, Dahlqvist M, Magnus F, Olafsson S, Arnalds U, Alling B, Abrikosov IA, Hjorvarsson B, Persson POÅ, Rosen J (2013) Magnetic self-organized atomic laminate from first principles and thin film synthesis. Phys Rev Lett 110:195502
8. Tao QZ, Hu CF, Lin S, Zhang HB, Li FZ, Qu D, Wu ML, Sun YP, Sakka Y, Barsoum MW (2014) Coexistence of ferromagnetic and a re-entrant cluster glass state in the layered quaternary $(Cr_{1-x}Mn_x)_2GeC$. Mater Res Lett. doi:10.1080/21663831.2014.909542
9. Mockute A, Persson POÅ, Magnus F, Ingason AS, Olafsson S, Hultman L, Rosen J (2014) Synthesis and characterization of arc deposited magnetic (Cr,Mn)$_2$AlC MAX phase films. Phys Status Solidi RRL 8(5):420–423
10. Ingason AS, Petruhins A, Dahlqvist M, Magnus F, Mockute A, Alling B, Hultman L, Abrikosov IA, Persson POÅ, Rosen J (2014) A nanolaminated magnetic phase: Mn_2GaC. Mater Res Lett 2:89–93